Endo:Press®

NIR / ICG FLUORESCENCE IMAGING IN THORACOSCOPIC SEGMENTECTOMY

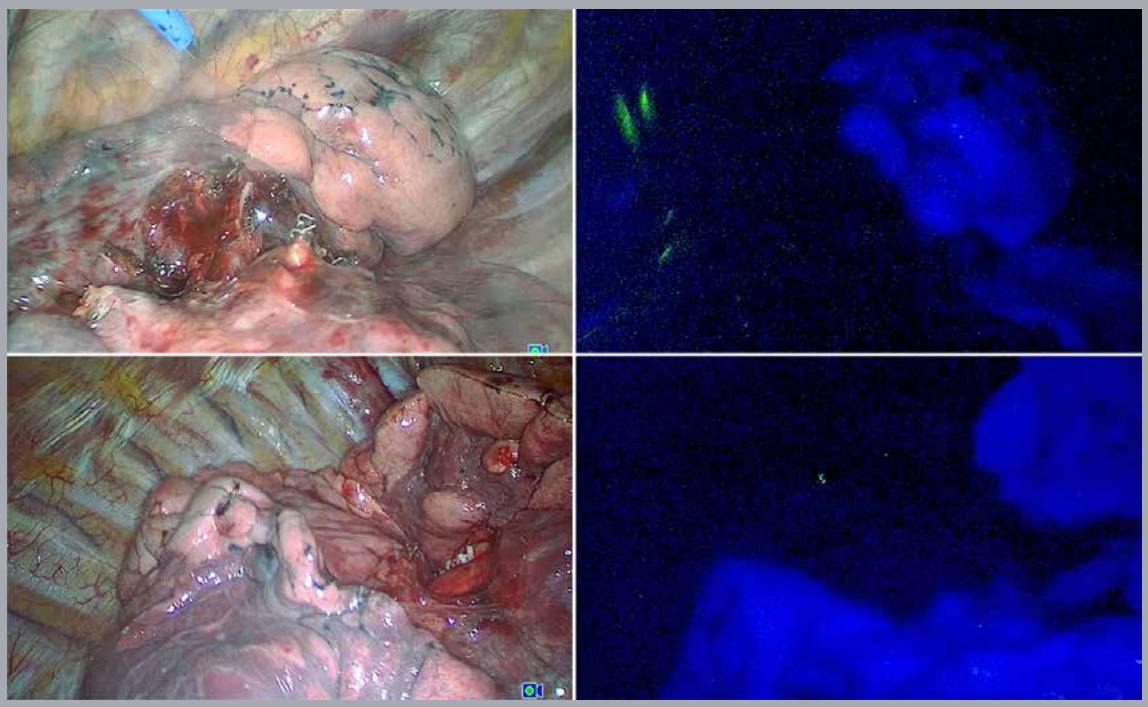

Vadim G. PISCHIK
Aleksandr I. KOVALENKO

Endo : Press®

NIR/ICG FLUORESCENCE IMAGING FOR THORACOSCOPIC SEGMENTECTOMY

Vadim G. PISCHIK[1]
Aleksandr I. KOVALENKO[2]

[1] I Professor, Thoracic Surgeon
Director, Center of Thoracic Surgery
[2] I MD, PhD Student

Medical Faculty of Saint Petersburg State University
Center of Thoracic Surgery
L.G. Sokolov Federal Hospital No. 122
Saint Petersburg, Russia

ICG / NIR-Fluorescence-Imaging for Thoracoscopic Segmentectomy

Vadim G. Pischik[1] and **Aleksandr I. Kovalenko**[2]

[1]| Professor, MD, Thoracic Surgeon
Director, Center of Thoracic Surgery
[2]| MD, PhD Student

Medical Faculty of Saint Petersburg State University
Center of Thoracic Surgery
L. G. Sokolov Federal Hospital No. 122
Saint Petersburg, Russia

Correspondence address:

Vadim Grigoryevich Pischik
D.m.n., Professor
Rukovoditel tsentra torakalnoy khirurgii
Klinicheskaya bolnitsa No. 122 im. *L. G. Sokolova*
194291 Sankt-Peterburg, pr. Kultury 4
Russian Federation
Phone: +7 (812) 919-07-49
Email: thorax122@med122.com

Important notes:

Medical knowledge is ever changing. As new research and clinical experience broaden our knowledge, changes in treatment and therapy may be required. The authors and editors of the material herein have consulted sources believed to be reliable in their efforts to provide information that is complete and in accord with the standards accepted at the time of publication. However, in view of the possibility of human error by the authors, editors, or publisher, or changes in medical knowledge, neither the authors, editors, publisher, nor any other party who has been involved in the preparation of this booklet, warrants that the information contained herein is in every respect accurate or complete, and they are not responsible for any errors or omissions or for the results obtained from use of such information. The information contained within this booklet is intended for use by doctors and other health care professionals. This material is not intended for use as a basis for treatment decisions, and is not a substitute for professional consultation and/or use of peer-reviewed medical literature.

Some of the product names, patents, and registered designs referred to in this booklet are in fact registered trademarks or proprietary names even though specific reference to this fact is not always made in the text. Therefore, the appearance of a name without designation as proprietary is not to be construed as a representation by the publisher that it is in the public domain.

The use of this booklet as well as any implementation of the information contained within explicitly takes place at the reader's own risk. No liability shall be accepted and no guarantee is given for the work neither from the publisher or the editor nor from the author or any other party who has been involved in the preparation of this work. This particularly applies to the content, the timeliness, the correctness, the completeness as well as to the quality. Printing errors and omissions cannot be completely excluded. The publisher as well as the author or other copyright holders of this work disclaim any liability, particularly for any damages arising out of or associated with the use of the medical procedures mentioned within this booklet.

Any legal claims or claims for damages are excluded.

In case any references are made in this booklet to any 3rd party publication(s) or links to any 3rd party websites are mentioned, it is made clear that neither the publisher nor the author or other copyright holders of this booklet endorse in any way the content of said publication(s) and/or web sites referred to or linked from this booklet and do not assume any form of liability for any factual inaccuracies or breaches of law which may occur therein. Thus, no liability shall be accepted for content within the 3rd party publication(s) or 3rd party websites and no guarantee is given for any other work or any other websites at all.

All rights reserved.
1st Edition
© 2018 Endo:Press® GmbH
P.O. Box, 78503 Tuttlingen, Germany
Phone: +49 (0) 74 61/1 45 90
Fax: +49 (0) 74 61/708-529
Email: endopress@t-online.de

No part of this publication may be translated, reprinted or reproduced, transmitted in any form or by any means, electronic or mechanical, now known or hereafter invented, including photocopying and recording, or utilized in any information storage or retrieval system without the prior written permission of the copyright holder.

Editions in languages other than English and German are in preparation. For up-to-date information, please contact Endo:Press® GmbH at the address shown above.

Design and Composing:
Endo:Press® GmbH, Germany

Printing and Binding:
Straub Druck+Medien AG
Max-Planck-Straße 17, 78713 Schramberg, Germany

05.18–0.2

ISBN 978-3-89756-942-3

Contents

The Authors

Vadim Grigorevich Pischik
Professor, MD, Thoracic Surgeon
Medical Faculty of Saint Petersburg State University
Director, Center of Thoracic Surgery
L. G. Sokolov Federal Hospital No. 122
Chief of Thoracic Surgery of the Saint Petersburg District

Alexandr Igorevich Kovalenko
Postgraduate Fellow, Department of Surgery
Medical Faculty of Saint Petersburg State University
Thoracic Surgeon
L. G. Sokolov Federal Hospital No. 122
Saint Petersburg, Russia

1 Fluorescence Imaging in Medicine

1.1 The Fluorescence Phenomenon

In 1852, George Gabriel Stokes described the mineral Fluorite as emitting blue light following exposure to ultraviolet light.[37,38] He called the phenomenon 'Fluorescence' and coined the term 'Fluorophores' for substances exhibiting this feature.

The property to emit fluorescence is very common in nature. The sensitivity of delocalized electrons in aromatic ring structures is responsible for this. Once light energy is absorbed by the fluorochrome's organic molecules, a promotion of delocalized electrons from a ground state to a higher energy level occurs. Upon return from excited singlet state to ground state, energy is emitted in the form of photons reaching the observer's eye as fluorescence. The emitted fluorescence is lower in energy because a part of the absorbed exciting light energy is converted to heat.

Aromatic ring structures are key components of biological substances such as DNA, proteins and sugars. Since the 1960s, the property of these substances to emit fluorescent light has been used for real-time fluorescence imaging in life sciences and medicine. The oldest known FDA-approved near-infrared (NIR) fluorescent dye used in medicine is indocyanine green (ICG).

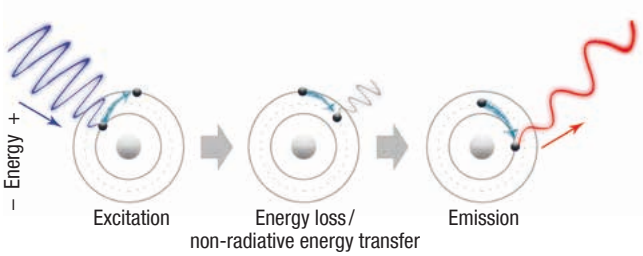

Fig. 1.1 Schematic drawing demonstrating the principle of fluorescence.

1.2 ICG and NIR Fluorescence

Indocyanine green is a fluorescent marker that has been used for decades in medicine. It was first approved by the FDA for angiographies in 1959 and is nowadays used for various types of applications. It is widely adopted for angiographies in ophthalmology and hepatology. Apart from being used to measure hepatic and cardiac function, it is applied in neurosurgical procedures.

ICG is composed of small particles that exhibit diffuse fluorescence when exposed to NIR excitation light (λ = 600 – 900 nm) delivered by a dedicated optical system. The absorption spectrum of the tricarbonate green dye shows an excitation peak at λ_{Ex} = 805 nm and a fluorescence emission peak at λ_{Em} = 835 nm. Owing to the inherent property of ICG to emit light in the NIR spectral range, there is virtually no interferring background autofluorescence arising from the main components of blood (hemoglobin and water). The resulting tissue penetration depth that can be used for detection of NIR fluorescence ranges from 0.5 cm – 1 cm.[31,32]

After intravenous injection, ICG binds to plasma proteins causing the agent to be confined within the intravascular space. The ICG protein complexes are then excreted in bile via the liver. The fluorescence of the bile can be used for real-time visualization of the extrahepatic bile ducts during NIR fluorescence cholangiography (FC).

Following submucosal injection, ICG is distributed in lymph where it binds to lipoproteins, and is drained via lymphatic pathways and nodes. In view of these characteristics, ICG lends itself to be used as a perfect marker for sentinel lymph node mapping.

The use of ICG is associated with a low risk of adverse effects. The risk of allergic reactions is one out of 42.000. For safety reasons, the use of ICG is contraindicated in patients with insufficient liver function and in those allergic to substances containing iodine, which is incorporated in the agent to a small fraction.[11] For the full range of contraindications, warnings, precautions, and adverse reactions related to the use of the drug, please refer to the manufacturer's instruction leaflet.

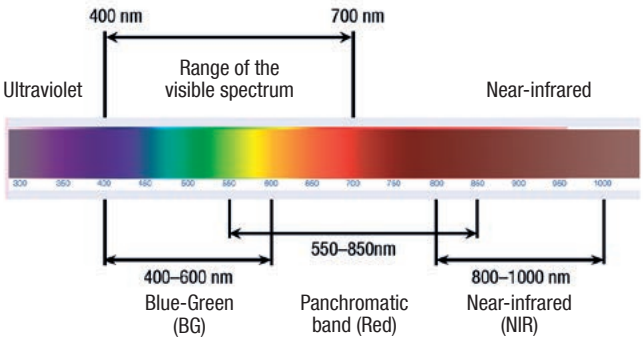

Fig. 1.2 Electromagnetic spectrum with close-up view of the visible and NIR wavelength ranges.

1.3. NIR Imaging Technology

All of the video stills presented in this brochure were captured using KARL STORZ OPAL1® technology for NIR/ICG imaging, which can be operated in a dual mode including both white-light (WL) and ICG-enhanced NIR fluorescence imaging. Apart from superb full HD image quality in WL mode and backlight illumination with true color gamut, the system offers a high level of user-friendly functionality. Switching from standard WL mode to NIR mode is simply done via foot-pedal control. Visualization in both modes is improved by use of the KARL STORZ IMAGE1 S™ platform offering various imaging modules which can be selected according to surgeon's preferences. The KARL STORZ OPAL1® technology for ICG-enhanced NIR fluorescence-guided procedures is fully compatible for extended applications such as 3D imaging, flexible endoscopy, and open surgery procedures (Fig. 1.3). For additional information, see the addendum section of this brochure, page 24.

Fig. 1.3 The KARL STORZ OPAL1® technology can be operated in a dual mode including both WL and ICG-enhanced NIR fluorescence-guided procedures.

2 Thoracoscopic Segmentectomy – An Alternative Option to Lobectomy

2.1 Introduction

Having been developed in the last decade, thoracoscopic surgery has become a mainstay in the treatment of thoracic cavity diseases. However, if a thoracic surgeon needs to perform more advanced surgeries, the loss of tactile sensation must be compensated with the use of augmented reality. Completeness of lymph node dissection, evaluation of organ perfusion, and delineation between lung segments are important factors which have propelled the demand for new modalities and concepts of visualization.

Fluorescence thoracoscopy with ICG has become a new method for creating augmented reality. The invention of the substance (ICG) dates back to the 1950s. Approximately 30 years ago, it had faded into oblivion and has recently been given a new lease on life. Due to the availability of video-endoscopic surgical equipment, which can display fluorescence emission after exposing the area of interest to light of the near-infrared range (NIR), surgeons are now able to see what has so far been invisible under standard WL conditions.

When injected into bloodstream, ICG allows detecting the blood supply of organs and tissues. Injected into the peritumoral space, the drug accumulates in the lymph nodes, thus allowing to track the lymphatic drainage pathways as well as to identify sentinel lymph nodes.

At the same time, the use of ICG-enhanced NIR fluorescence was not widely adopted in the field of thoracoscopic surgery, because procedures requiring this type of augmented visualization were rarely performed. Once it became clear, that there is a constant need for thoracoscopic segmentectomy,[23] thoracic surgeons began to reintroduce the dyes for appropriate intersegmental plane detection.

According to recent studies, thoracoscopic segmentectomy is an acceptable alternative to lobectomy for treating various lung diseases. This approach appears to provide equivalent rates of post-operative morbidity with potentially similar long-term results,[12] even in selected cases of lung cancer.[12,24,44] Obviously, the reduced extent of resection preserves lung parenchyma. This beneficial aspect has always played a major role in the surgical treatment of localized forms of bronchiectasis, pulmonary tuberculosis, and solitary pulmonary nodules. Alongside with that, the possibility to opt for a focal excision of malignant lung tumors has led to a fundamental rethinking of technical aspects of segmentectomy.

A prospective study from Japan found a statistically significant benefit in vital lung capacity (difference of 10 % on average) six months after lobectomy versus segmentectomy.[9] Other authors reported similar benefits, not only in terms of shorter chest tube duration, but also regarding the length of hospital stay after segmentectomy.[46] Preservation of the pulmonary parenchyma as well as minimal trauma to respiratory muscles are critical factors when defining the extent of resection and planning a surgical approach in patients with severe chronic obstructive pulmonary disease (COPD).[19] Moreover, segmentectomy is also essential for patients with multifocal lung carcinoma. *M. K. Bae et al.* (2011)[2] conducted a study on 40 patients and found no significant differences in the long-term outcomes of lobectomy and segmentectomy, but revealed significant benefits in the postoperative course of the segmentectomy group. In other studies dealing with the surgical treatment of synchronous primary lung carcinoma (SPLC), the authors showed that polysegmental resections do not worsen the long-term outcomes of treatment, possibly being a good alternative to lobectomy and

pneumonectomy.[18,40] A reasonable minimization of the removed parenchyma in oligometastatic lung nodules is just as important to the preservation of a patient's functional reserves. According to the *International Registry of Lung Metastases* from 1997, one-fifth of 5,206 patients subjected to metastasectomy required reoperation of other nodules, and 5 % of patients required three or more reoperations.[30] Despite the advanced chemotherapeutic drugs currently available, surgery is still a major contributing factor to the outcome of treatment in such patients.[43] Segmentectomy is considered to be safer than lobectomy both in terms of postoperative morbidity and mortality.[3] Apart from that, reducing the extent of resection to wedge resection is not always feasible and in some cases even counterproductive. In a study by *M. Higashiyama et al.* (2015),[10] 11 % of patients received a non-anatomical lung resection. Tumor cells were identified in the suture margin, which inevitably lead to local recurrence of disease. Segmentectomy allows lung resection to be performed as determined by anatomical boundaries, the identification of which is essential both for oncological and lung-sparing reasons.

2.2 Demarcation of Intersegmental Planes – A Survey of Methods

The success of thoracoscopic segmentectomy largely depends on the use of specific methods suited to determine the segmental lung anatomy.[14,21,27] One of the most complicated surgical steps of segmentectomy, besides intralobar lymph node dissection, is identification of the intersegmental planes. Both organ preservation and the degree of oncological radicality of rgw surgery are subject to proper determination of a segment's anatomical boundaries. The wrong interpretation of the invisible border between adjacent segments may potentially lead to unnecessary lung resection, positive surgical margins and even to a loss of the target in the remaining lung parenchyma. In this regard, the use of technical aids assisting in intersegmental plane formation during thoracoscopic segmentectomy is crucial.

In recent decades, various methods that can be used to identify intersegmental planes have been published. The test most commonly used in clinical practice involves inflating the lung after clamping the target bronchus in order to delineate the boundary between the inflated lung and the deflated target segment.[29] Some surgeons are focused on intersegmental veins when separating pulmonary parenchyma by sharp dissection.[25] Other experts perform contrast 'staining' of lung tissue through veins, arteries, and bronchi.[47] The above options are each associated with benefits and drawbacks. However, demarcation of intersegmental planes during ICG-enhanced NIR fluorescence-guided thoracoscopy is fundamentally different from a technical point of view.[13,21,41]

Next, we will discuss various ways of visualizing intersegmental boundaries.

2.2.1 Method No. 1: Creation of an Inflation / Deflation Line

Since the first segmentectomies were performed, a fairly simple and reproducible method to delineate intersegmental boundaries based on inflation and/or deflation of a target segment has been described.[7] However, inflation of the whole lung after clamping the segmental bronchus may spread air through the interalveolar pores (pores of Kohn), displace the intersegmental border and may obstruct vision.[29] Excessive inflation of non-ventilated lung areas, especially in patients with emphysema, makes it even more difficult to identify the exact intersegmental borders and resection margins.

Selective ventilation of the target segment could improve the validity of the method for thoracoscopy.[27] There are several variants of bronchial selective ventilation. One of them has been designed to show the boundaries of inflation / deflation: at first, the entire lung is inflated, then the bronchus of the target segment is ligated, and the lung is deflated. It is believed that deflation has only a minor collateral ventilation effect on intersegmental boundaries.[27] Technically, this can be performed using a clamp, a ligation loop, or a stapler that locked on the target bronchus.

Another option for selective ventilation of the target segment is using jet ventilation under bronchoscopic control.[29] During surgery, an endoscopist introduces a fiberoptic bronchoscope into the bronchus of the segment to be removed. Jet ventilation is performed through the instrument channel of the bronchoscope. Furthermore, a target segment can be inflated directly by placing a butterfly needle into the bronchus.[15] In conclusion, none of the above ventilation methods, with their varying degrees of complexity, allow to identify the intersegmental plane during thoracoscopy with adequate precision.

Conclusion on ventilation methods used to define intersegmental boundaries:

- **Benefits:** relative simplicity of application (inflation / deflation).
- **Drawbacks:** possible distortion of the true segmental boundaries, obscured thoracoscopic view, the need for additional traction, reducing the space for manipulations, lengthening surgery, need for additional instruments related to the use of a bronchoscope.

2.2.2 Method No. 2: Orientation Based on Anatomical Landmarks

During resection of the lung parenchyma, some surgeons trace relevant anatomical structures, particularly intersegmental veins, to identify intersegmental planes.[27] Dissection along the intersegmental vein can help to preserve the venous return from the remaining segments, which is essential in thoracic surgery. In 'old school' textbooks of thoracic surgery, the technique was recommended and widely used in combination with stripping of the parenchyma when applying traction on the segmental bronchus stump.[25] Enabling a relatively accurate delineation of intersegmental boundaries, the method is associated with bleeding caused by damage to small venous inflow tributaries. In the era of open surgery, this maneuver was facilitated by using gauze, allowing the surgeon to stop or reduce any bleeding by applying pressure. The resulting wound surface required separate treatment: coagulation of small sources of bleeding, suturing of sources of air leaks, etc. In thoracoscopy, use of this technique is hardly feasible.

In open surgery, such an approach was considered to be the only one available to remove posterior segments of the lower lobes due to the deep location of the target bronchus.[27] Despite the theoretically 'anatomic' way of the method, wide variability in the pulmonary venous anatomy significantly impedes any attempt of tracing landmarks for segmentectomy. Even after spotting an intersegmental vein, the abscence of landmarks on the visceral pleura does not permit the use of staplers. Provided the intersegmental vein is the only landmark to be followed by the surgeon, in the middle and superficial third of the intersegmental line, the use of sharp dissection is imperative. In modern thoracoscopy, this approach is more commonly used to determine hilar landmarks when the jaws of the endostapler are placed along the intersegmental veins to preserve the venous supply of the remaining lung tissue.

Conclusion on methods used to define intersegmental boundaries based on anatomical landmarks:

- **Benefits:** solidity of hilar boundaries.
- **Drawbacks:** inconvenient during thoracoscopy; lack of markers on the costal border surface requires stripping or coagulation along intersegmental vein; added need to use other imaging techniques and hemo-aerostasis.

2.2.3 Method No. 3: Dye Injection Technique

The method of injecting various dyes into the components of a root segment was developed when the need to perform segmentectomy became obvious. *S. Sugimoto et al.* (2010)[39] made use of an animal model to determine intersegmental boundaries by injecting indigo carmine into the pulmonary artery branches and bronchi of pigs. For the same purpose, other authors used methylene blue, which they instilled into segmental bronchi, arteries and veins of patients undergoing surgery.[47] Apart from that, the experience with intrabronchial injection of ICG for open segmentectomy was described.[26] While all of these methods allow defining the intersegmental lung boundaries with sufficient precision, they are associated with common drawbacks. First and foremost, there is an additional need to correctly address and manipulate the hilar components of a segment. This is critically determined by accurate distribution of the dye and requires highly accurate manipulations with strict control of injection depth and speed of performance. Commonly, the injection method requires a significant amount of dye, as in the absence of blood flow it is necessary to fill the vascular bed of the target segment. Apart from that, excessive delivery of dye may result in its redistribution and technical difficulties when removing the specimen. Administration of the dye into segmental pulmonary arteries is a time-consuming and not quite reliable method, especially when faced with segments perfused through several arteries.

With endobronchial administration, difficulties may arise related to the distribution of the dye in the bronchial tree caused by a significant amount of secretion. Thus, during surgical treatment of patients with inflammatory lung disease and in those suffering from COPD, the efficiency of endobronchial dye administration depends on the effectiveness of bronchial tree lavage.[47] The authors recommend this method for clinics with limited availability of surgical equipment.

Conclusion on injection methods used to define intersegmental boundaries:

- **Benefits:** solidity of boundaries.
- **Drawbacks:** depends on the precision of additional maneuvers to be performed in the course of dye injection; substantially greater amount of dye required; more time-consuming.

2.2.4 Method No. 4: Perfusion Assessment with ICG-Enhanced NIR Fluorescence Imaging

A fundamentally new solution is to define the boundaries of segments based on the perfused vs. non-perfused part of the lung parenchyma. In recent years, the use of a special dye – ICG – has gained in acceptance.[13,17,26,41] As discussed earlier, the dye can be delivered into bloodstream in various ways. The easiest way of administration is via systemic circulation through a peripheral or central vein following dissection of the bronchus and artery of the target segment. Once the dye passes into pulmonary circulation, fluorescence is detected in the perfused lung portion, whereas lack of the fluorescence signal is noticeable in the part to be removed because ICG has not entered it. The method obviates the need to ventilate the lung to be operated on, which significantly improves visualization during thoracoscopy, especially in cases of severe pulmonary emphysema. Potential adverse reactions to ICG (as laid down in the manufacturer's patient information sheet) are the only drawbacks of the method known so far. In early studies, it was demonstrated that the rate of anaphylactic reactions to ICG at a dose less than 0.5 mg/kg of body weight is 0.003 %, considerably increasing beyond the threshold of 5 mg/kg of body weight.[36] Modern optical systems allow to use the drug in much smaller amounts, which potentially reduces the risk of complications to zero.

Conclusion on perfusion methods used to define intersegmental boundaries:

- **Benefits:** solidity of boundaries; ease of application; freedom of manipulation during thoracoscopy; temporary clamping tests allows to check whether the lesion belongs to the target segment; subsegmental level.
- **Drawbacks:** possible allergic reactions (dose-dependent), the need for special equipment.

2.3. Thoracoscopic Segmentectomy with ICG-Enhanced NIR Fluorescence Imaging

2.3.1 Indications

In the past few years, thoracoscopic segmentectomy has gained in acceptance for the treatment of early stage non-small-cell lung cancer (NSCLC).[23] According to recently published data, the rate of NSCLC ranges from 55 % to 79 % among the overall number of thoracoscopic segmentectomies.[6,8,28] Less frequently, segmentectomy is the treatment of choice for metastatic lesions (16 %–21 %), benign tumors (12%), and inflammatory lung diseases (11 %). Irrespective of the need for organ-preserving surgery, it is, above all, necessary to identify the indications for curative treatment of the tumor.

The key issue in current debates is related to oncological efficiency of segmentectomy in patients with lung cancer. On the one hand, surgical treatment of non-invasive adenocarcinoma *(minimally invasive adenocarcinoma, MIA)* and adenocarcinoma in-situ *(in situ pulmonary adenocarcinoma, AIS)* is known to produce better long-term outcomes as compared to those of other morphological types of lung cancer.[42] AIS and MIA are tumors which practically do not metastasize. Therefore, one of the clinician's tasks is to identify such 'favorable' types of lung cancer during the preoperative workup. The prognostic criterion (*consolidation to tumor ratio – C/T*), defined on the basis of CT imaging as a ratio between the overall diameter of a lesion and its solid portion, has a specificity of 96.4 % when identifying tumors with a favorable prognosis.[1] Apart from that, patient survival also depends on the size of the lesion, with the boundary indicator for segmentectomy equal to 2 cm.[33] Unlike the surgical treatment of solitary metastases,[10] the use of wedge resections in NSCLC patients is associated with a poor long-term outcome.[35] Furthermore, according to the study by *B. G. Leshnower et al*. (2010)[20], the safety marging of parenchymal resection in segmentectomy must be at least 2 cm from any tumor.

The existing evidence for the safe and effective use of segmentectomy in the surgical treatment of lung cancer can be summarized in the following table based on the publication by *C. Yang* and *T. D'Amico* (2014).[45]

- **Indications of BTC segmentectomy in lung cancer:**
  - The size of the lesion is less than 2 cm
  - C/T < 0.25; GGO; AIS or MIA
- **Conditions:**
  - The safety margin of resection should be no less than the diameter of the lesion.
  - Sufficient volume of lymph node dissection (intralobal and mediastinal)
- **Benefits:**
  - Not inferior in terms of oncologic radicality compared to lobectomy preserving the parenchyma
  - Better long-term results than wedge resections
- **Future studies:**
  - Analyzing and defining the efficiency in the treatment of lesions ranging from 2 to 3 cm
  - Excluding restrictions related to comorbidities
  - Identification of morphological tumor types amenable to curative resection.

Explanation of abbreviations:
Consolidation to tumor ratio (C/T); ground-glass opacity (GGO); in situ pulmonary adenocarcinoma (AIS); minimally invasive adenocarcinoma (MIA).

The increasing rate of segmentectomies for the treatment of metastatic lung cancer – reported since 1980 – ranges from 3 % to 23 %, and seems to be related to a broad agreement about the importance of preserving the parenchyma.[3] Segmentectomy with solitary lung metastases is recommended in conditions where wedge resection is technically not feasible and lobectomy redundant.[10] Deep metastases and groups of lesions in a single anatomical structure are optimal for segmentectomy. The decision-making in choosing segementectomy over wedge resection for the treatment of peripheral metastases has not been studied sufficiently. However, wedge resection of a peripheral node without a sufficient resection margin is considered an additional indication for segmentectomy.[10]

Surgery also plays a crucial role in the treatment of inflammatory lung diseases. In the operative treatment of specific (tuberculosis, mycobacteriosis, aspergillosis) and nonspecific (bronchiectasis, chronic abscesses) lung lesions, the surgeon has to achieve a complete removal of the lesion while preserving as much functional lung tissue as possible. The solution to this problem is segmentectomy.[16,22,34] The indication for surgery in the complex treatment of localized forms of inflammatory diseases is determined by the following conditions:

- Failure of drug therapy (resistance, intolerance).
- Risk of recurrence of infection and/or, other associated complications (pulmonary hemorrhage).

In addition, it is believed that small lung neoplasms suggestive of malignancy also need to be removed with segmentectomy.[8] If primary lung cancer is confirmed by intraoperative frozen section histology, wedge resection seems to be non-radical while subsequent segmentectomy results in an elaborate task. This partially explains the group of benign neoplasms among segmentectomies in the published data.[6,8,28]

Thus, the indications for thoracoscopic segmentectomy include the following:

- Non-small-cell lung cancer of IA stage with a tumor size of less than 2 cm as well as a C/T ratio of less than 0.25.
- Deep location of a metastatic lung lesion or identification of a group of metastatic nodes in one segment.
- In cases where the resection margin would be too close to the tumor if wedge resection would be chosen.
- Localized forms of inflammatory pulmonary disease.

2.3.2 Preoperative Workup and Patient Selection

All candidates for thoracoscopic segmentectomy need to undergo a standard preoperative assessment similar to that of other anatomical lung resections. The workup includes laboratory examinations assessing the function of internal organs and indicators of blood clotting and hematopoiesis. First of all, it is necessary to evaluate the cardiopulmonary reserves. In their study, *M. F. Berry et al.* (2011)[4] demonstrated that unlike thoracotomy, a thoracoscopic approach is an eligible option for patients with lower functional reserves. Segmentectomy, by nature, also offers benefits over lobectomy in preserving the parenchyma.[46] However, no recommendations modifying the borderline indications for thoracoscopic resection and anatomical segmentectomy in particular have been issued yet. In this regard, the surgeon must decide whether patients with a high postoperative risk and a smaller volume should be elected for segmentectomy despite a mismatch with regard to standard recommendations. Some authors consider such conditions an additional indication for segmentectomy.[6,8] In our clinical practice, thoracic specialists use an examination algorithm that includes a pulmonary function test (body plethysmography) and echocardiography, and if necessary, cardiopulmonary exercise tests.[5]

All candidates with a confirmed diagnosis of primary lung cancer require an integrated chest PET-CT for N-staging. Patients with metastatic lung lesions routinely undergo examinations to exclude local recurrence of the primary tumor.

2.3.3 Step-by-Step Approach to Videothoracoscopic Segmentectomy with ICG-Enhanced NIR Fluorescence Imaging

The most important component of the preoperative planning for thoracoscopic segmentectomy is imaging of the vascular anatomy of the lung. It is necessary to elucidate and determine the course of both arteries and veins. The authors use 3D modeling of the lung by reconstructing i.v. contrast-enhanced CT scans for preoperative planning. The hilar anatomy of a patient is analyzed as well as the relative topography of lesions. For this purpose OsiriX MD for the Mac operating system and the RadiAnt DICOM Viewer for the Windows operating system are used (Fig. 2.1). The role of preoperative modeling will be clearly demonstrated in *Patient No. 3,* Chapter 3: *'Clinical Case Histories'*.

In the authors' clinical practice, thoracoscopic segmentectomy routinely involves the use of a two-port approach: One incision of up to 2–3 cm in length is made in the 5th intercostal space, with the center along the anterior axillary line. The second incision is 1 cm in length and placed in the 7–8th intercostal space along the middle axillary line (Fig. 2.2). The scope used for thoracoscopy is 10 mm in diameter with a viewing angle of 30°. Thoracoscopy is performed using OPAL1® technology for NIR/ICG fluorescence imaging (KARL STORZ Tuttlingen, Germany), necessitating a cold light source equipped with a special filter for emission of NIR light. During exposure and isolation of hilar segmental structures, a precise dissection of lymph node stations 11, 12, and 13 is performed (Fig. 2.3). Next, the vessels are ligated with plastic clips, and a stapler is applied to the bronchus. Once ligation or transection of arterial and bronchial structures of the target segment is complete, the anesthesiologist is allowed a bolus injection of ICG solution.

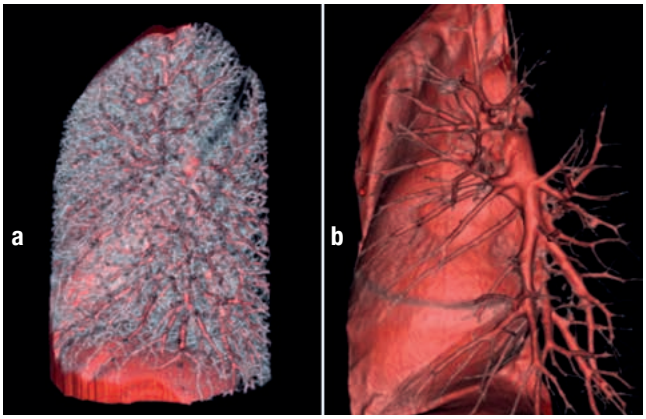

Fig. 2.1 Preoperative 3D modeling of the left lung (primary lung cancer S1–2 of the left lung).

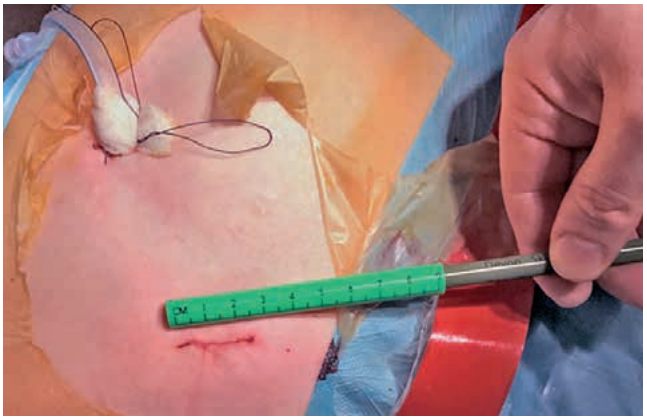

Fig. 2.2 Two-port thoracoscopic approach used for segmentectomies.

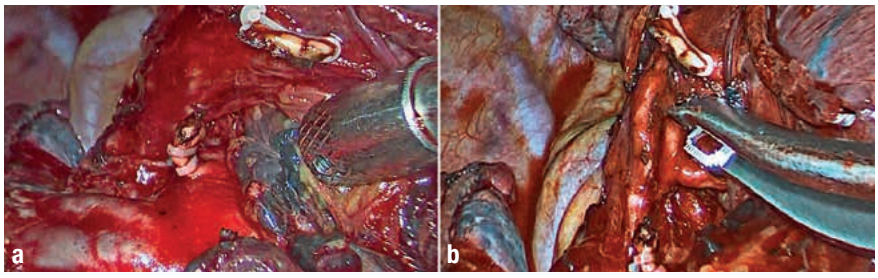

Fig. 2.3 Intraoperative views prior to (**a**) and after (**b**) of level-1 lymph node dissection of stations 11, 12 and 13 (the artery of the 2nd segment is clipped and transected).

ICG is diluted immediately before administration using 10 ml of water for injection. Thus, a diluted preparation of 2.5 mg per ml of solution is obtained (10 ml of the solution contains 25 mg of ICG). Based on our experience with ICG, the following conclusions about the dose and technique of administration are drawn:

1. The starting dose of the dye should be about 0.15 mg/kg of body weight, i.e. 4 to 5 ml of solution. This volume is absolutely sufficient to obtain fluorescence of the lung portion being perfused. The rest of the solution can be used later if fluorescence-guided visualization of the segment needs to be repeated.
2. The dye can be injected either into the peripheral vein or into the central catheter (superior vena cava, subclavian, jugular vein). The time before emission of fluorescence depends on the way of injection. Once a bolus of ICG solution has been injected into a central vein, fluorescence occurs within 1–3 seconds after administration. When injected into a peripheral vein, fluorescence appears within 10–15 seconds after administration. It is important for the surgeon to be aware of the time frame available and to be readily prepared to mark the boundary (e.g., by electrocautery spots), as well as to prepare the thoracoscope, switch on the video camera, and the light source which is set to NIR/ICG mode beforehand.
3. It should be noted that the anatomical structures of the target segment as well as the key intrathoracic landmarks are practically invisible while operating in NIR mode. Both the anatomical boundaries of the surgical site and the fluorescent boundaries can be controlled while toggling between WL mode and NIR mode by use of a foot-pedal switch or via the control button on the camera head. Among the specific visualization modes offered by the camera system (Image1 S™ technology, KARL STORZ Tuttlingen, Germany), our surgical team prefers using the one which creates an intense bright blue or green glow radiating from the perfused areas.
4. The effective duration of fluorescence is 30 to 120 seconds. The time frame depends on the severity of emphysema as well as on the degree of lung collapse and collateral circulation. Once the available time has expired, luminescence may spread beyond the target segment due to retrograde blood flow along the intersegmental veins.
5. If the surgeon is in doubt about the accuracy of the highlighted boundaries of the target segment, administration of ICG can be repeated, but not earlier than 15 minutes later. In this time interval, a significant decrease in luminescence intensity of the lung parenchyma occurs. After administration of the next bolus of the drug, despite the residual fluorescence, the intensity of enhancement in the perfused lung portion will increase, and within a minute, the boundaries of the perfused segments will be clearly visible.

Examples of the detection of perfusion boundaries are shown in Figs. 2.4-2.8.

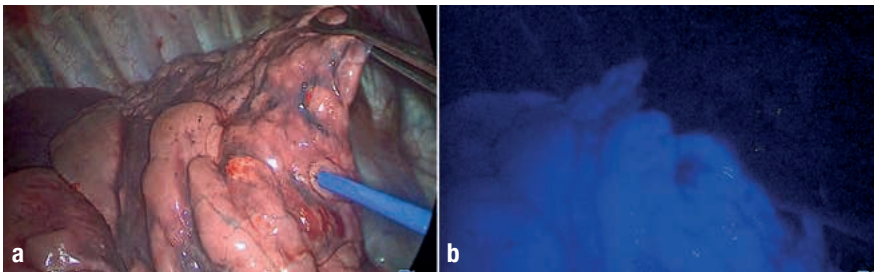

Fig. 2.4 Intraoperative images taken during WL mode (**a**) and NIR mode (**b**) used to define the intersegmental boundaries for right lung segmentectomy S1.

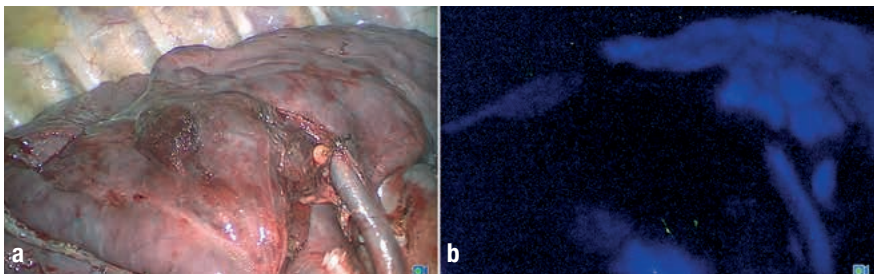

Fig. 2.5 Intraoperative images taken during WL mode (**a**) and NIR mode (**b**) used to define the intersegmental boundaries for right lung segmentectomy S3.

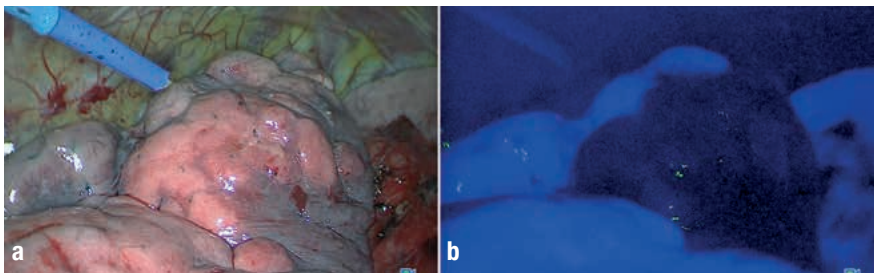

Fig. 2.6 Intraoperative images taken during WL mode (**a**) and NIR mode (**b**) used to define the intersegmental boundaries for left lung segmentectomy S1–2.

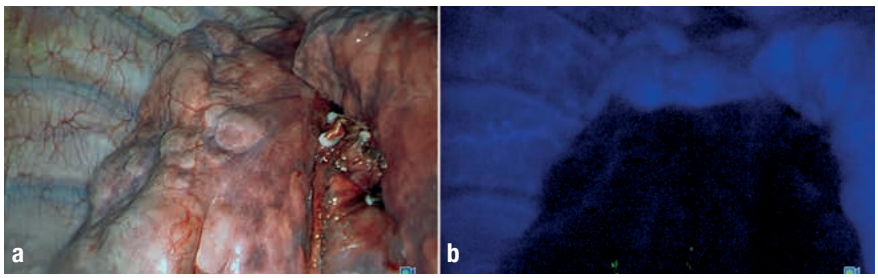

Fig. 2.7 Intraoperative images taken during WL mode (**a**) and NIR mode (**b**) used to define the intersegmental boundaries for right lung segmentectomy S7–10.

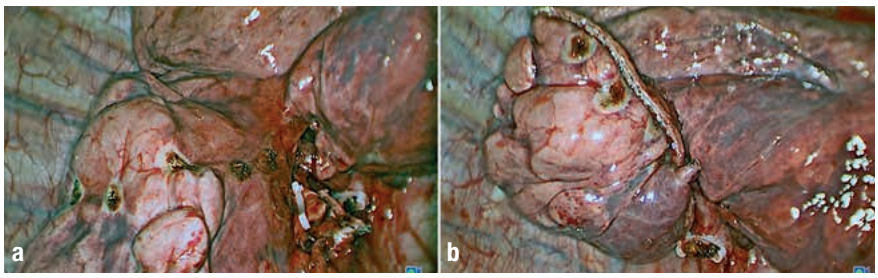

Fig. 2.8 Intraoperative images taken before (**a**) and after (**b**) the resection of basilar segments of the right lung.

Fig. 2.9 Intraoperative image showing an intersegmental boundary which is marked with electrocautery.

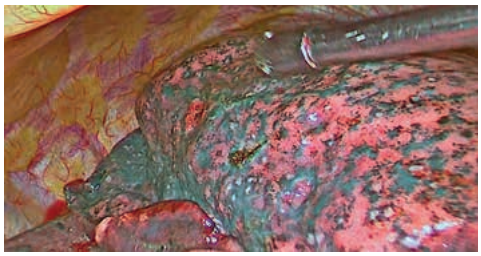

Fig. 2.10 Intraoperative image showing a comparison of both techniques used to define the intersegmental boundary: ventilation (inflated segment) and perfusion (indicated by electrocautery dots).

Once anatomical boundaries – highlighted by ICG-enhanced NIR fluorescence – between the target segments to be removed and those to be preserved have been marked by electrocautery (Fig. 2.9), the division of lung parenchyma is the next step to take. For comparison, it is possible to perform a ventilation test while ligating the segmental bronchus (Fig. 2.10). The transection is carried along the identified intersegmental boundaries. For this purpose, we prefer the use of endostaplers. Special attention should be paid to the selection of the correct stapler cartridge. Most commonly, the use of cartridges with a staple height for thick tissue (color code: green or purple) is recommended, except for particular cases with thin layers of the pulmonary parenchyma (where a blue cartridge is advisable). The stapler should be positioned along the marked boundaries on the costal and mediastinal surface of the lung, aligned toward the hilum of the resected segment. Care must be taken to ensure that the central stumps of the transected bronchus and vessels are proximal to the stapled suture line and that the peripheral stumps are inside the surgical specimen of the target segment. Thus, with correct cleavage of the intersegmental plane, two staple lines surrounding the hilum of the target segment are created (Fig. 2.11). Any surgery performed on a patient with a malignant tumor is complemented by a lobe-specific mediastinal lymph node dissection of at least 3 groups of lymph nodes, with the obligatory inclusion of station 7 (Fig. 2.12).

Fig. 2.11 Image of a surgical specimen (posterior segment of the superior lobe of the right lung: segmental vessels are ligated with plastic clips, the segmental bronchus stump is shown after stapling; the resection lines of the parenchyma encircle the hilum of the target segment).

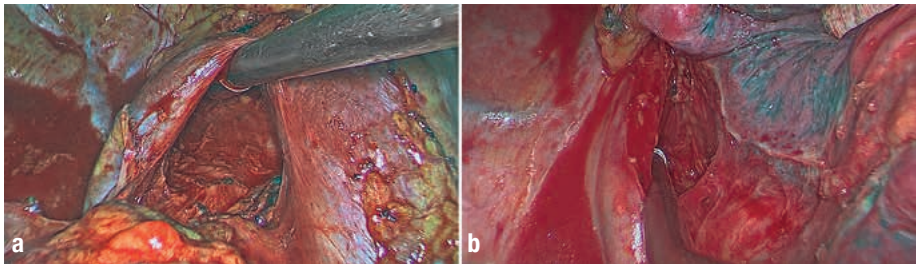

Fig. 2.12 Intraoperative images of level-2 lymph node dissection of stations 2R–4R (**a**) and station 7 (**b**).

2.3.4 ICG-Enhanced NIR Fluorescence Imaging for Ligation of the Segmental Pulmonary Artery

During segmentectomy, the surgeon needs to check if the vessel belongs to that part of the lobe in which the target lesion is located. This is facilitated if the lesion is amenable to palpation or visualization on the surface.

In this case, we recommend marking the target lesion with monopolar electrocoagulation to facilitate its identification on the surface, and to perform temporary vessel occlusion afterwards.

For this purpose, the target artery is isolated with a vessel loop. For its temporary occlusion, either a double turn of a sling (Fig. 2.13) or vascular bulldog clamp is used (Fig. 2.14). After occlusion of the vessel, 1–2 ml of ICG solution is injected into the central vein. Lack of fluorescence in the area of the lesion suggests that the clamped vessel actually perfuses the target site, and the artery can be transected at that point (Fig. 2.15).

If the lesion is located between two segments (Fig. 2.16), the surgeon has to change the surgical plan.

The above technique of temporary vessel occlusion is effective for segments which are perfused by one artery (e.g., S6, S7–10, S3, S8). Removing S2 on the right or S1–2 on the left, requires that at least two vessels be transected in advance. If the surgeon has not completely blocked the blood supply of the segment, the dye can spread into the target segment and identification of the intersegmental plane will fail. Most often, this occurs during segmentectomy S2 on the right, when the surgeon has missed to clamp the descending artery of the second segment, but still injects the dye. At the same time, one should be familiar with the hazards linked to the potential occurrence of technical flaws during vessel occlusion: the vessel (Fig. 2.17) has not been fully clamped, or the vessel is isolated at an overly distal position (subsegmental artery instead of segmental artery). In such cases, the pulmonary tissue around the lesion will exhibit fluorescence, and delineation of the intersegmental plane will be ineffective.

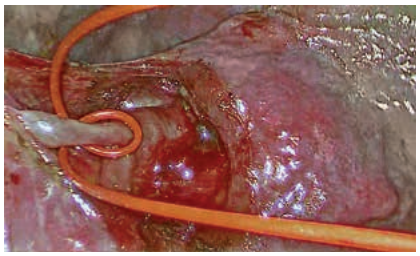

Fig. 2.13 Intraoperative image of temporary ligation of the artery of the 8th segment by double turnover of a sling.

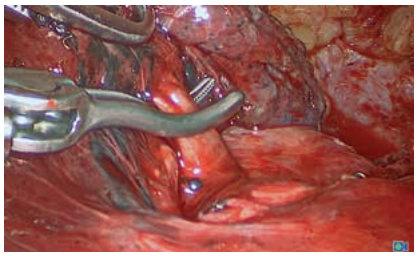

Fig. 2.14 Intraoperative image of temporary ligation of the artery of the 2nd segment using a vascular bulldog clamp.

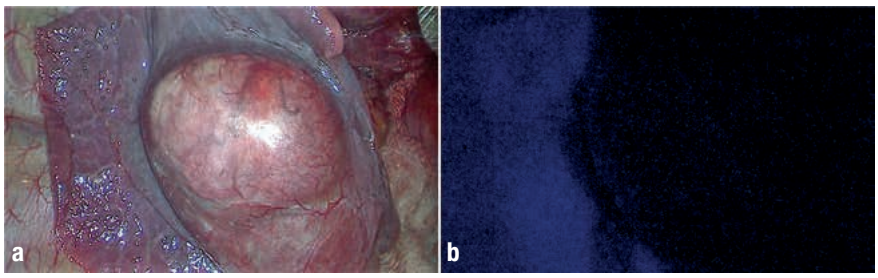

Fig. 2.15 Intraoperative images taken during WL mode (**a**) and NIR mode (**b**) after temporary occlusion of the artery of the 8th segment (metastasis from uterine leiomyoma is entirely located in the segment to be removed).

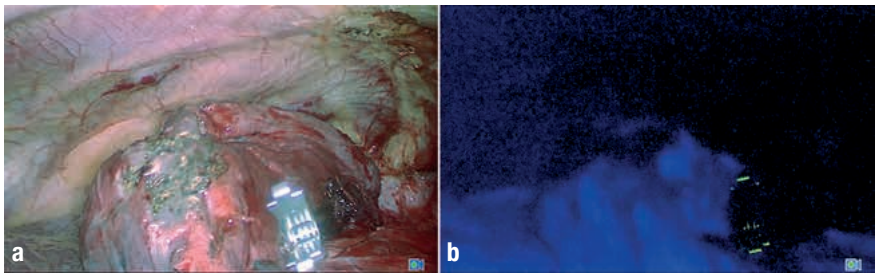

Fig. 2.16 Intraoperative images taken during WL mode (**a**) and NIR mode (**b**) after temporary occlusion of the subsegmental artery S1–2 on the left side (the lesion marked by monopolar coagulation is located on the boundary highlighted by fluorescence).

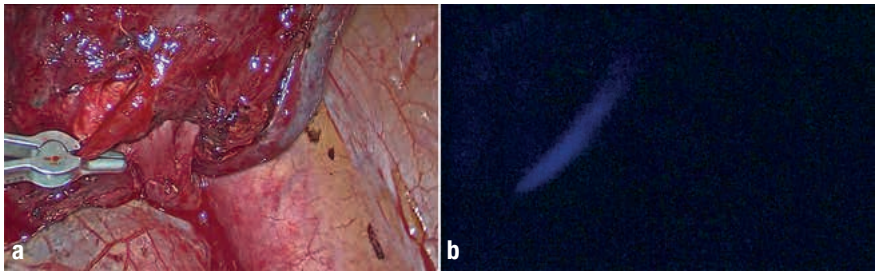

Fig. 2.17 Intraoperative images taken during WL mode (**a**) and NIR mode (**b**) after incomplete temporary occlusion of the artery (the blood flow in the vessel is maintained – visually confirmed by fluorescence).

The dose of ICG solution injected to locate a suitable site of occlusion should be significantly lower than the one used to define an intersegmental boundary. If a vessel has been selected wrongly by the surgeon, it will take a long time for the drug to be washed out of the lobe. In this case, administration of 1–2 ml of ICG solution allows to note the absence of fluorescence in the target segment while avoiding the 'over-enhancement' of the lung tissue. The insignificant fluorescence which remains in the lung tissue will not prevent the surgeon from locating intersegmental boundaries in the next 'enhancement phase' after bolus administration of a larger dose of ICG.

2.3.5 Limitations of the Technique

A few years ago, the main limitations of ICG-enhanced NIR fluorescence imaging in thoracoscopy were considered to be overly high doses of ICG and low intensity of contrast luminescence in patients with pulmonary emphysema.[41] Currently, advanced videoendoscopic equipment and surgical devices allow the use of minimal volumes of ICG solution, which reduces the risk of side effects and allows the drug to be re-administered in doubtful cases, including pulmonary emphysema.

3 Clinical Case Histories

Patient No. 1

The 64-year-old patient 'A.' presented for follow-up control after surgical treatment of papillary adenocarcinoma of the thyroid gland $pT_2N_0M_0$. At first CT scans of the chest taken in axial and frontal planes through the posterior segment of the right upper lobe (also termed 2nd segment) revealed irregular opacification of GGO type with substantial inclusions measuring 13 x 11 x 10 mm (Fig. 3.1). Using whole-body PET-CT, a solitary focus of abnormal uptake intensity of the 18-FDG (SUV – 4.2) was detected on cross-sectional planes through the pathological lesion; the lymph nodes of the mediastinum were of normal size.

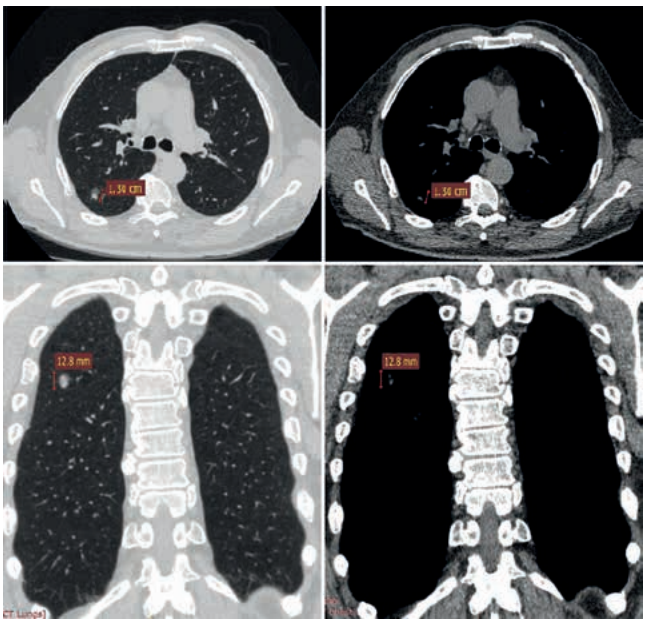

Fig. 3.1 CT scans of the chest organs in pulmonary and mediastinal modes with lesion of the posterior segment of the right lung.

Upon admission to hospital, the patient complained about a rare paroxysmal cough with scanty mucous sputum and a feeling of fatigue. At the time of admission, withdrawal from tobacco use dated back 6 years, however, with a prior history of more than 40 pack-years. No significant comorbidities based on functional and laboratory tests were found. There were no contraindications for operative treatment. There were no known allergic reactions to iodine-containing drugs. Considering the size and site of the lesion, its density, and metabolic activity, the patient was selected for thoracoscopic segmentectomy S2 of the right lung with lobe-specific lymph node dissection.

To determine the blood supply of the posterior segment of the right upper lobe, 3D reconstruction of the right lung vessels was performed using the RadiAnt Dicom Viewer program, version 3.4.2 (Fig. 3.2). A single artery of the 2nd segment was identified in a typical location on the border, along with two other arteries. The descending artery of the 2nd segment could not be determined reliably. Additional arteries supplying the lesion from adjacent segments were not detected.

Fig. 3.2 3D reconstruction of the segmental anatomy of vessels of the right lung (visualized artery of the 2nd segment, perfusing the tumor, and two arteries of the 6th segment).

Thoracoscopic surgery was performed using a standard two-port approach, as described above, under endotracheal anesthesia with separate intubation and single-lung ventilation. During visual inspection, the pleural cavity did not show any fluid or adhesions. The oblique interlobar fissure was partially complete. The hilar lymph nodes of the right lung were not enlarged. Upon instrumental palpation of the costal surface of the 2nd segment, close to the interlobar fissure, a dense, rounded lesion, approximately 1 cm in diameter, with puckered edges, was identified, with no signs of pleural involvement. The division of the oblique interlobar fissure was initiated from its midpoint, above the vessels. The endostapler was inserted into the tunnel created between the two arteries of the 6th and 2nd segments, resulting in the division of the parenchyma (Fig. 3.3).

The artery of the 2nd segment was isolated by a rubber sling, then clipped, and transected (Fig. 3.4). Dissection of bronchial structures was continued. During lymph node dissection of the intralobal trifurcation, the bronchi of the apical, posterior, and anterior segments of the right upper lobe were visualized (Fig. 3.5). The bronchus of the 2nd segment was isolated, followed by its transection using the endostapler. The cold light source was then adjusted to NIR/ICG mode. Next, 5 ml of 2.5 % solution of ICG were injected into the central vein. Immediately after ICG administration, all of the lung tissue except for the 2nd segment appeared with bright blue fluorescence. The anticipated resection line was marked by monopolar coagulation along the visible boundary on the costal and interlobar surface (Fig. 3.6). A bright blue fluorescence was observed for the first 30 seconds. Then, along with the mosaic-like diffusion to the target segment, fluorescence gradually faded away about 4 minutes

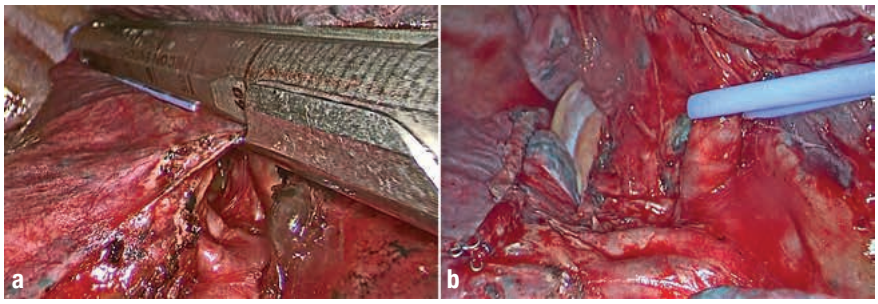

Fig. 3.3 Intraoperative images showing division of the posterior half of the oblique interlobar fissure which is guided by the 2nd-segment artery and two arteries of the 6th segment.

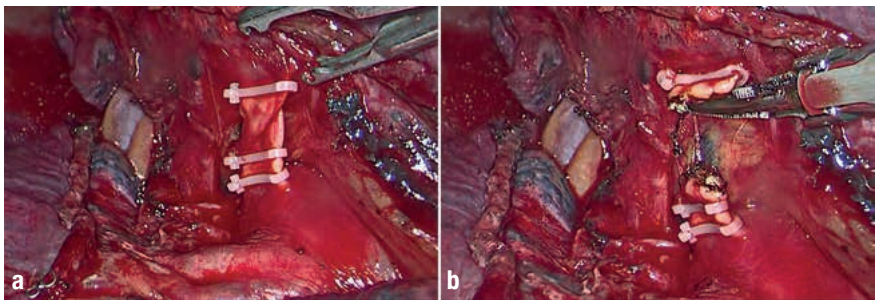

Fig. 3.4 Intraoperative images showing the clipping (**a**) and transection (**b**) of the artery of the 2nd segment (shown are the peribronchial lymph nodes of the superior lobe).

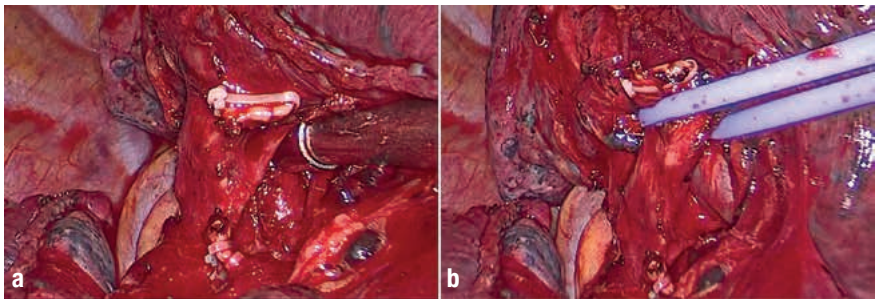

Fig. 3.5 Intraoperative images of lymph node dissection of the intralobal trifurcation of the superior lobe bronchus. The lymph nodes are completely removed, embedded in the specimen. The bronchus of the posterior segment is grasped with a holder, the bronchus of the apical segment and the bronchus of the anterior segment are visualized.

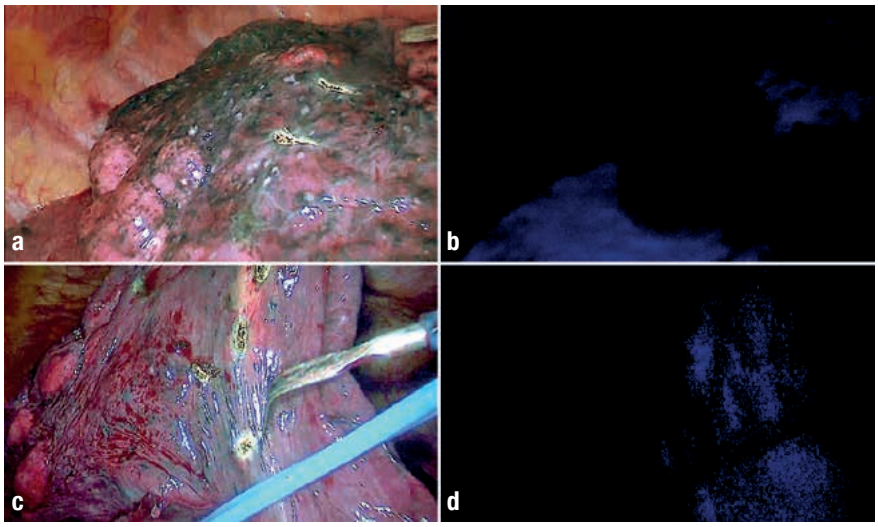

Fig. 3.6 Intraoperative images showing the anticipated boundary (marked with electrocautery dots) for resection of the second segment which is demonstrated along the costal surface (**a, b**) and from the side of the interlobar fissure (**c, d**).

after administration. Division of the branches of the superior pulmonary vein was followed by ligation and transection of the primary vein of the 2nd segment. The intersegmental branches were preserved (Fig. 3.7). Four green endostapler cartridges were applied to resect the posterior segment along the marked lines. The peripheral stumps of artery, vein, and bronchus were included in the surgical specimen (Fig. 3.8). The specimen was extracted from the pleural cavity in a sealed endobag. A cross-section of the tumor sample showed indistinct edges of dirty-gray color with dark inclusions. Afterwards, the paratracheal and bifurcation lymph nodes were dissected (Fig. 3.9). The surgery was concluded with the placement of a pleural drainage tube passed through the rear port and up to the apex of the pleural cavity. The duration of surgery was 150 minutes. Overall surgical blood loss was 30 ml. A macroscopic view of the extracted specimen of the 2nd segment, harboring the peripheral tumor, is shown in Fig. 3.10.

The postoperative period was uneventful. The chest tube was removed on postoperative day 2. The patient was discharged on postoperative day 3. Based on histopathological analysis, the neoplasm was reported to be a primary pulmonary non-invasive adenocarcinoma. No signs of malignancy were found in either resection margin or any of the 16 lymph nodes.

Fig. 3.7 Intraoperative image taken after clipping and transection of the vein of the 2nd segment with preservation of intersegmental branches.

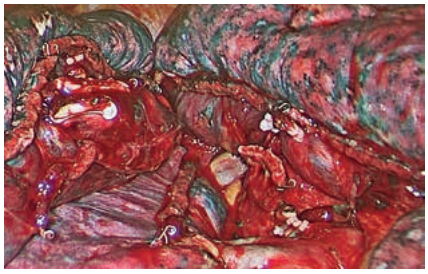

Fig. 3.8 Intraoperative image after resection of the posterior segment (the stumps of the artery and vein of the 2nd segment are clipped, the stumps of the bronchus are treated with a stapler).

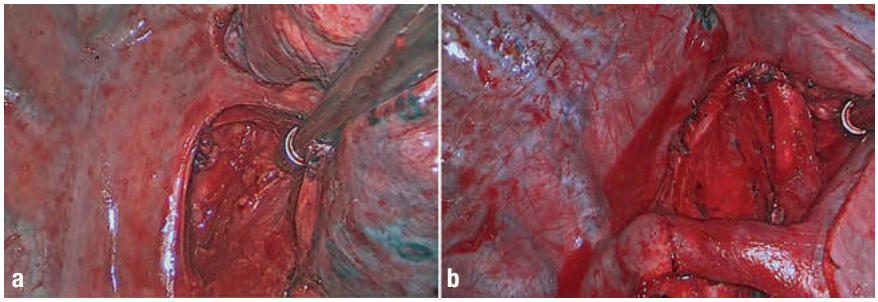

Fig. 3.9 Intraoperative images of lymph node dissection of the bifurcation group (**a**) and paratracheal group (**b**).

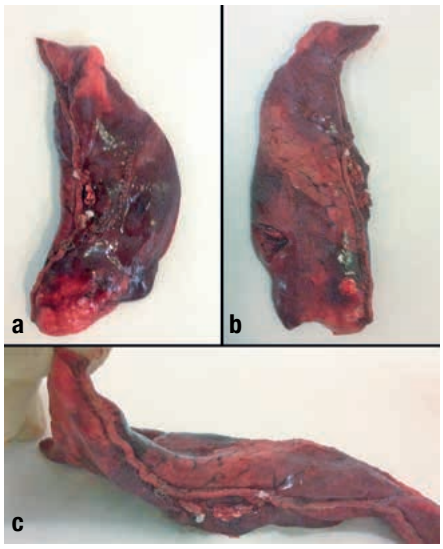

Fig. 3.10 Macroscopic views of a surgical specimen extracted from the 2nd segment of the right lung harboring a tumor. Rear aspect (**a**), anterior view (**b**), and lateral view of the lung root (**c**).

Patient No. 2

The 38-year-old female patient K. reported that – since her childhood – she had received advanced conservative treatment for bronchiectatic disease. After suffering from severe left lower lobe pneumonia, during the past two years, exacerbations of the disease flared up more intensively. Despite ongoing treatment, persisting disorders were as follows: subfebrile temperature, general weakness, and cough with copious expectoration of purulent sputum. She started complaining about mild hemoptysis and, after examination and treatment in the pulmonary department, she was referred to us for consultation with the thoracic surgery team. Based on the chest CT, localized bronchiectasis of the basilar pyramid and lingular segments of the left lung were identified (Fig. 3.11). No signs of bronchiectasis in the remaining segments of the left and right lungs were found.

The patient's history showed neither harmful habits nor any known allergic reactions to medications. Based on the pulmonary function test, the vital capacity was at the lower limit of reference range with normal forced expired volume in 1 second. No other comorbidities were revealed.

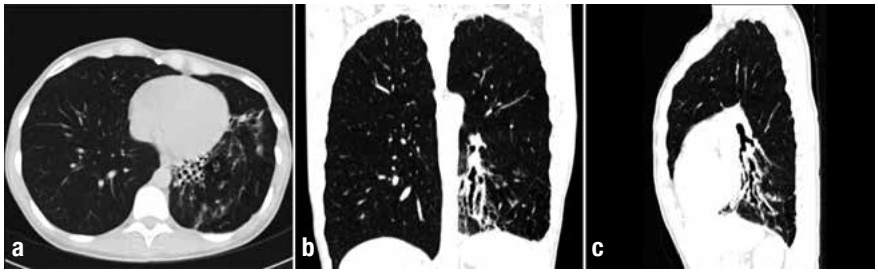

Fig. 3.11 Preoperative chest CT in three cross-sectional planes (localized bronchiectasis of the basilar pyramid and lingular segments).

Taking the clinical course and CT findings into account, the patient was scheduled to undergo VATS 'transverse' resection of the left lung (polysegmentectomy of the basilar segments [S8–10] and lingual segments [S4–5]). 3D reconstruction of the left lung vasculature and bronchi was performed and did not reveal any arterial abnormalities. At the same time, enlarged lymph nodes and convoluted bronchial arteries were found.

The double-port thoracoscopic procedure was performed under general anesthesia in right decubitus position. Thoracoscopic exploration showed clearly visible fissures with adhesions in the anterior part. The posterior surface of the lower lobe showed fibrous alterations and was adherent to the chest wall and lingular segments. The adhesions were lysed with an ultrasonic scalpel (Fig. 3.12). We noticed perivascular and peribronchial fibrosis of the hilum as well as multiple enlarged lymph nodes measuring up to 2–3 cm in diameter (Fig. 3.13).

The inferior pulmonary ligament was divided up to the level of the inferior pulmonary vein. Two convoluted, hypertrophic bronchial arteries (Fig. 3.14) were transected with an ultrasonic scalpel. Following dissection of the enlarged lymph node conglomerate from the side of the interlobar fissure (Fig. 3.15), branches from the pulmonary artery were exposed. The arteries of the lingular and basilar segments were transected after clipping.

The segmental veins (V4–5; V8–10) were treated in a similar way while preserving the intersegmental branches. Lingular and basilar bronchi were transected using two green endostapler cartridges. After that, in order to determine the perfusion

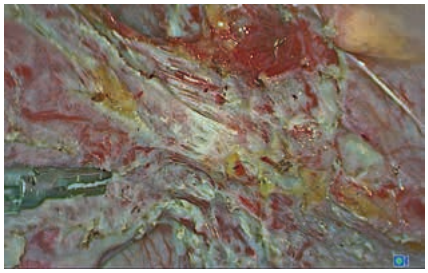

Fig. 3.12 Intraoperative image showing lysis of adhesions between the fibrously altered lower lobe of the left lung and the chest wall.

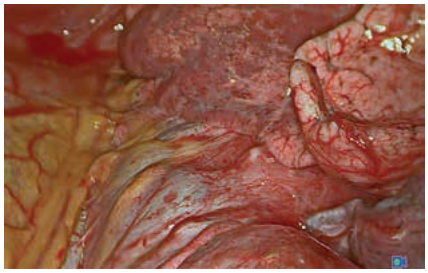

Fig. 3.13 Intraoperative image demonstrating perivascular and peribronchial fibrosis of the hilum and multiple enlarged lymph nodes.

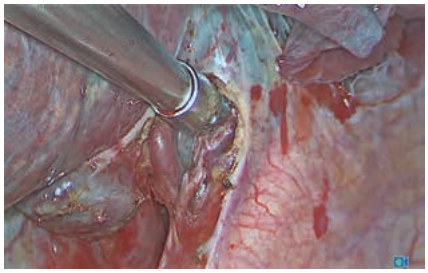

Fig. 3.14 Intraoperative image of hypertrophic bronchial arteries after dissection of the inferior pulmonary ligament.

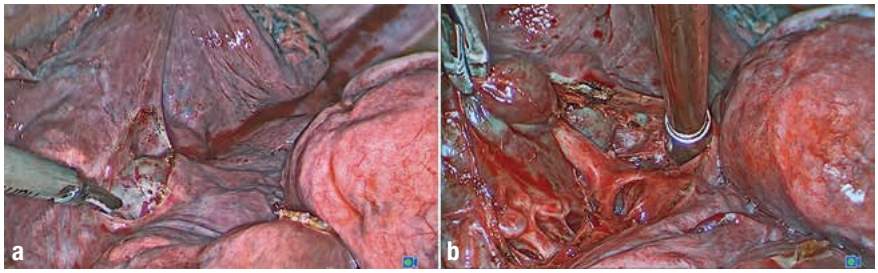

Fig. 3.15 Intraoperative view of lymphadenopathy in the depth of the interlobar fissure (**a**). View of the dissected branches of the pulmonary artery (**b**).

boundaries of the anticipated resection line, ICG solution was injected twice in the central vein with an interval of 15 minutes (Fig. 3.16). Based on the boundaries marked in advance with electrocautery dots, two segmental resection maneuvers were performed consecutively with the stapler fired five times (blue cartridge), and two times (green cartridge) (Fig. 3.17). The surgery was completed with insertion of a 24-Fr. chest drain, passed through the rear port to the apex of the pleural cavity, followed by complete re-expansion of the remaining segments. The duration of the procedure was 250 minutes, and overall blood loss was 50 ml.

There were no complications during the postoperative period. The patient was discharged on postoperative day 6. No health-related problems were revealed at 3-month follow-up. The chest CT scans of that particular follow-up are shown in Fig 3.18.

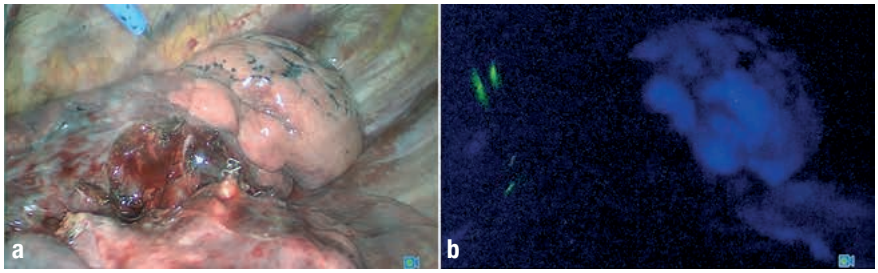

Fig. 3.16 Intraoperative images taken during WL mode (**a**) and NIR mode (**b**) for delineation of intersegmental boundaries followed by 'transverse' resection of the left lung (fluorescence S1–3 and S6 of the left lung is noticeable).

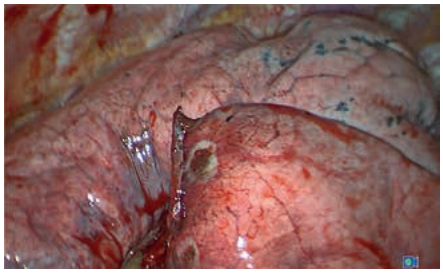

Fig. 3.17 Intraoperative image after 'transverse' resection of the left lung.

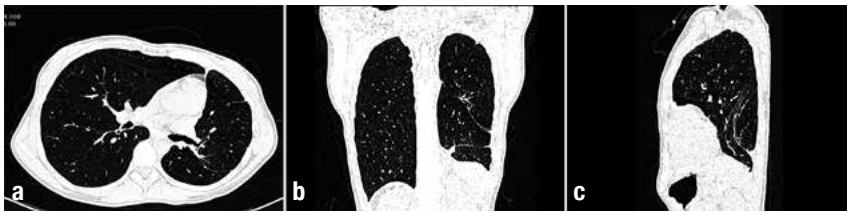

Fig. 3.18 Postoperative CT scans of the thorax in transverse (**a**), frontal (**b**) and sagittal planes (**c**).

Patient No. 3

The 78-year-old female patient was referred to us one year after radical surgery for the treatment of adenocarcinoma of the middle-ampullar rectum $pT_3N_0M_0$. A solitary metastasis located in the 6th segment of the right lung was found. According to PET-CT imaging, no other foci of pathology-related FDG radiotracer uptake were found. No signs of local recurrence of the primary tumor were found neither by pelvis MRI nor by endoscopic examination. Due to the deep location of the metastatic nodule, the patient was scheduled to undergo right thoracoscopic segmentectomy S6.

3D modeling of hilar elements of the right lung was performed, revealing abnormalities of the arterial and venous vasculature of the 6th segment. The vein of the 6th segment was drained into the right superior pulmonary vein (Fig. 3.19a). Apart from that, the artery of the 6th segment was found to give off an additional ascending artery in the 2nd segment (Fig. 3.19b).

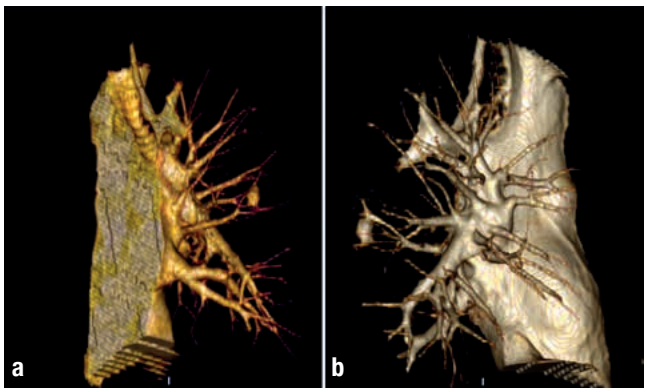

Fig. 3.19 3D reconstruction of segmental anatomy of the vessels of the right lung.

a. Shown is the vein of the 6th segment, draining into the right superior pulmonary vein.

b. An additional ascending artery of the 6th segment is given off in the 2nd segment.

The surgical procedure was performed based on the standard protocol described above. The interlobar fissure was partly complete. There were no signs of adhesions or fluid in the pleural cavity. Following division of the inferior pulmonary ligament and dissection of station 7 lymph nodes, the vein of the 6th segment was seen to pass to the superior pulmonary vein (Fig. 3.20). Subsequently, interlobar dissection was initiated. Using a predefined landmark (an artery of the 6th segment with a branch to the 2nd segment), a tunnel was formed above the arterial vasculature. The parenchyma was divided with the endostapler (Fig. 3.21). At this point, the artery of the 6th segment was isolated distally as far as the additional A2 branch, and clipped (Fig. 3.22). In the next step, a bolus of ICG solution was injected into a central vein (Fig. 3.23) after transecting the bronchus and vein of the 6th segment. The resulting bright fluorescence allowed to delineate the intersegmental boundaries. However, immediately after this, fluorescence rapidly spread to the target segment, which most certainly was caused by an arterial abnormality. The parenchyma was divided along the previously marked dots. The surgery was completed with the insertion of a 24-Fr. chest drain passed through the rear port to the apex of the pleural cavity. The duration of the procedure was 90 minutes, and the overall blood loss was 20 ml.

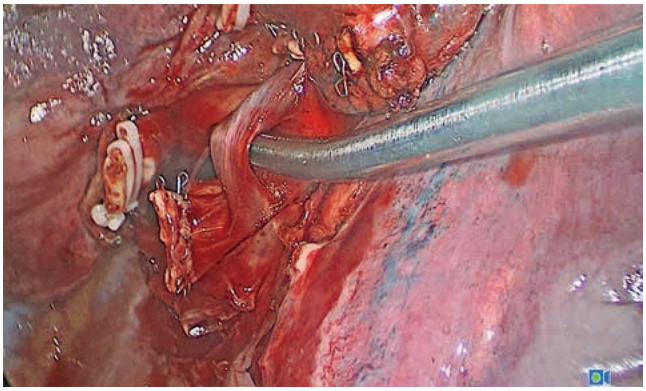

Fig. 3.20 Intraoperative image of the vein of the 6th segment separated, which drains into the superior pulmonary vein.

No complications occurred during the post-operative period. The patient was discharged on postoperative day 4.

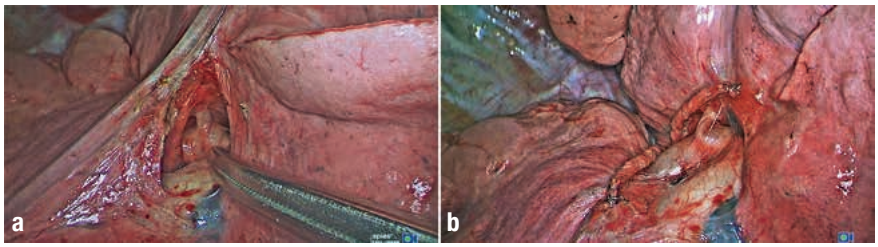

Fig. 3.21 Intraoperative images showing the formation of a tunnel (**a**) and intersection of the intersegmental S2–S6 planes. Dissection was guided by the 6th segmental artery and a thin branch of the 2nd segment (**b**).

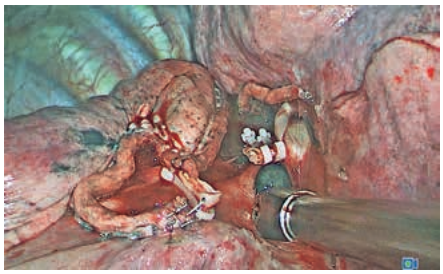

Fig. 3.22 Intraoperative image showing transection of the 6th segmental artery while preserving integrity of the artery of the 2nd segment.

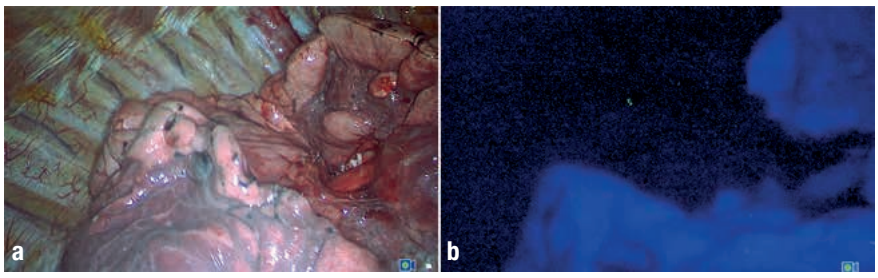

Fig. 3.23 Intraoperative images taken during WL mode (**a**) and NIR mode (**b**) for delineation of intersegmental boundaries of the 6th segment of the right lung.

4 Conclusion

Summarizing all of the above statements and experiences, the use of NIR/ICG technology is considered a safe and effective method to elucidate and determine the individual patient's lung anatomy, which is of high importance for the planning of resection margins during thoracoscopic segmentectomies. Using a state-of-the-art endoscopic system allows to reduce the potential risks of side effects associated with the use of the drug itself and the dose administered. Doubling the dose of ICG allows clear detection of the intersegmental plane, even under suboptimal circumstances.

5 References

1. ASAMURA H, HISHIDA T, SUZUKI K, KOIKE T, NAKAMURA K, KUSUMOTO M et al. Radiographically determined noninvasive adenocarcinoma of the lung: survival outcomes of Japan Clinical Oncology Group 0201. J Thorac Cardiovasc Surg 2013;146(1):24–30.
2. BAE MK, BYUN CS, LEE CY, LEE JG, PARK IK, KIM DJ et al. The role of surgical treatment in second primary lung cancer. Ann Thorac Surg 2011;92(1):256–62.
3. BERRY MF. Role of segmentectomy for pulmonary metastases. Ann Cardiothorac Surg 2014;3(2):176–82.
4. BERRY MF, ONAITIS MW, TONG BC, HARPOLE DH, D'AMICO TA. A model for morbidity after lung resection in octogenarians. Eur J Cardiothorac Surg 2011;39(6):989–94.
5. BRUNELLI A, KIM AW, BERGER KI, ADDRIZZO-HARRIS DJ. Physiologic evaluation of the patient with lung cancer being considered for resectional surgery: Diagnosis and management of lung cancer, 3rd ed: American College of Chest Physicians evidence-based clinical practice guidelines. Chest 2013;143(5 Suppl):e166S-e190S.
6. CERFOLIO RJ, WATSON C, MINNICH DJ, CALLOWAY S, WEI B. One Hundred Planned Robotic Segmentectomies: Early Results, Technical Details, and Preferred Port Placement. Ann Thorac Surg 2016;101(3):1089-95; Discussion 1095-6.
7. CHURCHILL ED, BELSEY R. Segmental pneumonectomy in bronchiectasis: the lingula segment of the left upper lobe. Ann Surg 1939;109(4):481–99.
8. DEMIR A, AYALP K, OZKAN B, KABA E, TOKER A. Robotic and video-assisted thoracic surgery lung segmentectomy for malignant and benign lesions. Interact Cardiovasc Thorac Surg 2015;20(3):304–9.
9. HARADA H, OKADA M, SAKAMOTO T, MATSUOKA H, TSUBOTA N. Functional advantage after radical segmentectomy versus lobectomy for lung cancer. Ann Thorac Surg 2005;80(6):2041–5.
10. HIGASHIYAMA M, TOKUNAGA T, NAKAGIRI T, ISHIDA D, KUNO H, OKAMI J. Pulmonary metastasectomy: outcomes and issues according to the type of surgical resection. Gen Thorac Cardiovasc Surg 2015;63(6):320–30.
11. HOPE-ROSS M, YANNUZZI LA, GRAGOUDAS ES, GUYER DR, SLAKTER JS, SORENSON JA et al. Adverse reactions due to indocyanine green. Ophthalmology 1994;101(3):529–33.
12. HWANG Y, KANG CH, KIM H, JEON JH, PARK IK, KIM YT. Comparison of thoracoscopic segmentectomy and thoracoscopic lobectomy on the patients with non-small cell lung cancer: a propensity score matching study. Eur J Cardiothorac Surg 2015;48(2):273–8.
13. IIZUKA S, KURODA H, YOSHIMURA K, DEJIMA H, SETO K, NAOMI A et al. Predictors of indocyanine green visualization during fluorescence imaging for segmental plane formation in thoracoscopic anatomical segmentectomy. J Thorac Dis 2016;8(5):985–91.
14. IWATA H, SHIRAHASHI K, MIZUNO Y, MATSUI M, TAKEMURA H. Surgical technique of lung segmental resection with two intersegmental planes. Interact Cardiovasc Thorac Surg 2013;16(4):423–5.
15. KAMIYOSHIHARA M, KAKEGAWA S, IBE T, TAKEYOSHI I. Butterfly-needle video-assisted thoracoscopic segmentectomy: a retrospective review and technique in detail. Innovations (Phila) 2009;4(6):326–30.
16. KANG M, KIM HK, CHOI YS, KIM K, SHIM YM, KOH W et al. Surgical treatment for multidrug-resistant and extensive drug-resistant tuberculosis. Ann Thorac Surg 2010;89(5):1597–602.
17. KASAI Y, TARUMI S, CHANG SS, MISAKI N, GOTOH M, GO T et al. Clinical trial of new methods for identifying lung intersegmental borders using infrared thoracoscopy with indocyanine green: comparative analysis of 2- and 1-wavelength methods. Eur J Cardiothorac Surg 2013;44(6):1103–7.
18. KOCATURK CI, GUNLUOGLU MZ, CANSEVER L, DEMIR A, CINAR U, DINCER SI et al. Survival and prognostic factors in surgically resected synchronous multiple primary lung cancers. Eur J Cardiothorac Surg 2011;39(2):160–6.
19. LAU KKW, MARTIN-UCAR AE, NAKAS A, WALLER DA. Lung cancer surgery in the breathless patient--the benefits of avoiding the gold standard. Eur J Cardiothorac Surg 2010;38(1):6–13.
20. LESHNOWER BG, MILLER DL, FERNANDEZ FG, PICKENS A, FORCE SD. Video-assisted thoracoscopic surgery segmentectomy: a safe and effective procedure. Ann Thorac Surg 2010;89(5):1571–6.
21. MISAKI N, CHANG SS, IGAI H, TARUMI S, GOTOH M, YOKOMISE H. New clinically applicable method for visualizing adjacent lung segments using an infrared thoracoscopy system. J Thorac Cardiovasc Surg 2010;140(4):752–6.
22. MITCHELL JD, YU JA, BISHOP A, WEYANT MJ, POMERANTZ M. Thoracoscopic lobectomy and segmentectomy for infectious lung disease. Ann Thorac Surg 2012;93(4):1033-9; discussion 1039-40.
23. NAKAMURA K, SAJI H, NAKAJIMA R, OKADA M, ASAMURA H, SHIBATA T et al. A phase III randomized trial of lobectomy versus limited resection for small-sized peripheral non-small cell lung cancer (JCOG0802/WJOG4607L). Jpn J Clin Oncol 2010;40(3):271–4.
24. NOMORI H, MORI T, IKEDA K, YOSHIMOTO K, IYAMA K, SUZUKI M. Segmentectomy for selected cT1N0M0 non-small cell lung cancer: a prospective study at a single institute. J Thorac Cardiovasc Surg 2012;144(1):87–93.
25. NOMORI H, OKADA M. Illustrated Anatomical Segmentectomy for Lung Cancer. Tokyo: Springer Japan; 2012. (ISBN No. 978-4-431-54143-1).
26. OH S, SUZUKI K, MIYASAKA Y, MATSUNAGA T, TSUSHIMA Y, TAKAMOCHI K. New technique for lung segmentectomy using indocyanine green injection. Ann Thorac Surg 2013;95(6):2188–90.
27. OIZUMI H, KATO H, ENDOH M, INOUE T, WATARAI H, SADAHIRO M. Techniques to define segmental anatomy during segmentectomy. Ann Cardiothorac Surg 2014;3(2):170–5.

28. OJANGUREN A, GOSSOT D, SEGUIN-GIVELET A. Division of the intersegmental plane during thoracoscopic segmentectomy: is stapling an issue? J Thorac Dis 2016;8(8):2158–64.

29. OKADA M, MIMURA T, IKEGAKI J, KATOH H, ITOH H, TSUBOTA N. A novel video-assisted anatomic segmentectomy technique: selective segmental inflation via bronchofiberoptic jet followed by cautery cutting. J Thorac Cardiovasc Surg 2007;133(3):753–8.

30. PASTORINO U, BUYSE M, FRIEDEL G, GINSBERG RJ, GIRARD P, GOLDSTRAW P et al. Long-term results of lung metastasectomy: prognostic analyses based on 5206 cases. J Thorac Cardiovasc Surg 1997;113(1):37–49.

31. SCHAAFSMA BE, MIEOG JSD, HUTTEMAN M, VAN DER VORST, JOOST R, KUPPEN PJK, LOWIK, CLEMENS W G M et al. The clinical use of indocyanine green as a near-infrared fluorescent contrast agent for image-guided oncologic surgery. J Surg Oncol 2011;104(3):323–32.

32. SCHOLS RM, BOUVY ND, VAN DAM RM, STASSEN LPS. Advanced intraoperative imaging methods for laparoscopic anatomy navigation: an overview. Surg Endosc 2013;27(6):1851–9.

33. SCHUCHERT MJ, ABBAS G, AWAIS O, PENNATHUR A, NASON KS, WILSON DO et al. Anatomic segmentectomy for the solitary pulmonary nodule and early-stage lung cancer. Ann Thorac Surg 2012;93(6):1780-5; discussion 1786-7.

34. SHIRAISHI Y. Surgical treatment of nontuberculous mycobacterial lung disease. Gen Thorac Cardiovasc Surg 2014;62(8):475–80.

35. SMITH CB, SWANSON SJ, MHANGO G, WISNIVESKY JP. Survival after segmentectomy and wedge resection in stage I non-small-cell lung cancer. J Thorac Oncol 2013;8(1):73–8.

36. SPEICH R, SAESSELI B, HOFFMANN U, NEFTEL KA, REICHEN J. Anaphylactoid reactions after indocyanine-green administration. Ann Intern Med 1988;109(4):345–6.

37. STOKES GG. On the change of refrangibility of light. Philosophical Transactions of the Royal Society of London 1852(142):463–562.

38. STOKES GG. On the change of refrangibility of light II. Philosophical Transactions of the Royal Society of London 1853(143):385–96.

39. SUGIMOTO S, OTO T, MIYOSHI K, MIYOSHI S. A novel technique for identification of the lung intersegmental plane using dye injection into the segmental pulmonary artery. J Thorac Cardiovasc Surg 2011;141(5):1325–7.

40. TANVETYANON T, FINLEY DJ, FABIAN T, RIQUET M, VOLTOLINI L, KOCATURK C et al. Prognostic factors for survival after complete resections of synchronous lung cancers in multiple lobes: pooled analysis based on individual patient data. Ann Oncol 2013;24(4):889–94.

41. TARUMI S, MISAKI N, KASAI Y, CHANG SS, GO T, YOKOMISE H. Clinical trial of video-assisted thoracoscopic segmentectomy using infrared thoracoscopy with indocyanine green. Eur J Cardiothorac Surg 2014;46(1):112–5.

42. TRAVIS WD, BRAMBILLA E, NOGUCHI M, NICHOLSON AG, GEISINGER K, YATABE Y et al. International Association for the Study of Lung Cancer/American Thoracic Society/European Respiratory Society: international multidisciplinary classification of lung adenocarcinoma: executive summary. Proc Am Thorac Soc 2011;8(5):381–5.

43. TREASURE T, MILOSEVIC M, FIORENTINO F, MACBETH F. Pulmonary metastasectomy: what is the practice and where is the evidence for effectiveness? Thorax 2014;69(10):946–9.

44. WOLF AS, RICHARDS WG, JAKLITSCH MT, GILL R, CHIRIEAC LR, COLSON YL et al. Lobectomy versus sublobar resection for small (2 cm or less) non-small cell lung cancers. Ann Thorac Surg 2011;92(5):1819-23; discussion 1824-5.

45. YANG CJ, D'AMICO TA. Open, thoracoscopic and robotic segmentectomy for lung cancer. Ann Cardiothorac Surg 2014;3(2):142–52.

46. ZHANG L, MA W, LI Y, JIANG Y, MA G, WANG G. Comparative study of the anatomic segmentectomy versus lobectomy for clinical stage IA peripheral lung cancer by video assistant thoracoscopic surgery. J Cancer Res Ther 2013;9 Suppl 2:S106-9.

47. ZHANG Z, LIAO Y, AI B, LIU C. Methylene blue staining: a new technique for identifying intersegmental planes in anatomic segmentectomy. Ann Thorac Surg 2015;99(1):238–42.

Recommended Instrumentation and Imaging Systems for NIR / ICG Fluorescence Imaging for Thoracoscopic Segmentectomy

OPAL1® Technology for NIR / ICG

based on the IMAGE1 S™ camera system

① **IMAGE1 S™**
- brilliant FULL HD image quality
- NIR/ICG fluorescence in standard mode or SPECTRA A* mode

② **NIR/ICG telescope and camera head**
- 3-chip FULL HD camera head with high resolution, optimal NIR light sensitivity
- telescopes for optimal fluorescence excitation and detection; can be used for white light and fluorescence modes
- telescopes with various lengths and diameters

③ **D-LIGHT P light source (Xenon light source)**
- best daylight spectrum in white light and fluorescence modes
- no additional security measures (vs. Laser)
- with enhanced background display

④ **Footswitch**
- fast switch between white light and fluorescence mode

⑤ **Autoclavable fiber optic light cable**
- optimal light transmission in the white light and NIR spectral range

* *SPECTRA A:* **Not for sale in the U.S.**

It is recommended to check the suitability of the product for the intended purpose prior to use.

OPAL1® Technology for NIR / ICG

based on the IMAGE1 S™ camera system

Camera system

IMAGE1 S CONNECT™
TC 200

Camera control unit

IMAGE1 S™ H3-LINK
TC 300

Light source

D-LIGHT P / 20 1337 01-1
Spare lamp: **20** 1330 28
Lamp module: **20** 1337 25

Camera head

H3-Z FI
TH 102

Light cables

Fiber Optic Light Cables
495 NAC / NCSC / TIP / NCS / VIT

Telescopes

HOPKINS® Telescope
26003 ACA / BCA
26046 ACA / BCA

Open surgery

VITOM® II ICG
20 9160 25 AGA
Accessories:
28272 UGN / CN
28272 HC
28172 HR / HM

HOPKINS® Telescopes
for NIR/ICG Fluorescence Imaging

Diameter 10 mm, length 31 cm
Trocar size 11 mm

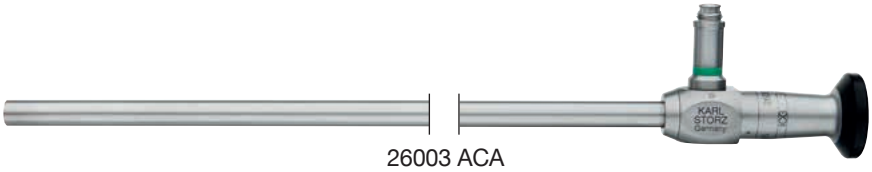

26003 ACA

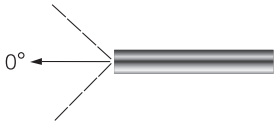

26003 ACA

HOPKINS® Straight Forward Telescope 0°,
enlarged view, diameter 10 mm, length 31 cm, **autoclavable**, for indocyanine green (ICG), fiber optic light transmission incorporated, for use with Fiber Optic Light Cable 495 NCSC, Fluid Light Cable 495 FQ/FR and Cold Light Fountain D-LIGHT P SCB **20**133701-1,
color code: green

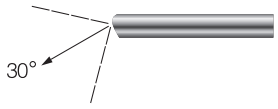

26003 BCA

HOPKINS® Forward-Oblique Telescope 30°,
enlarged view, diameter 10 mm, length 31 cm, **autoclavable**, for indocyanine green (ICG), fiber optic light transmission incorporated, for use with Fiber Optic Light Cable 495 NCSC, Fluid Light Cable 495 FQ/FR and Cold Light Fountain D-LIGHT P SCB **20**133701-1,
color code: red

Diameter 5 mm, length 29 cm
Trocar size 6 mm

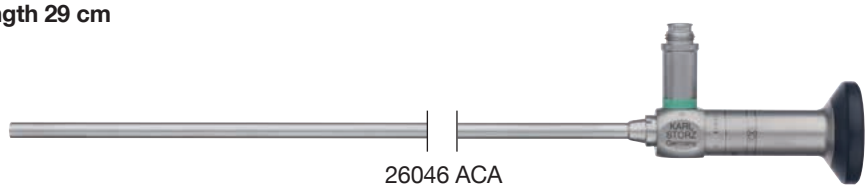

26046 ACA

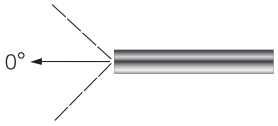

26046 ACA

HOPKINS® Straight Forward Telescope 0°,
enlarged view, diameter 5 mm, length 29 cm, **autoclavable**, for indocyanine green (ICG), fiber optic light transmission incorporated, for use with Fiber Optic Light Cable 495 NAC, H3-Z FI camera head and Cold Light Fountain D-LIGHT P SCB **20**133701-1,
color code: green

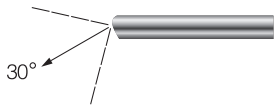

26046 BCA

HOPKINS® Forward-Oblique Telescope 30°,
enlarged view, diameter 5 mm, length 29 cm, **autoclavable**, for indocyanine green (ICG), fiber optic light transmission incorporated, for use with Fiber Optic Light Cable 495 NAC, H3-Z FI camera head and Cold Light Fountain D-LIGHT P SCB **20**133701-1,
color code: red

Instruments for Video-Assisted Thoracoscopic Surgery (VATS)

Basic Set

40160 CD	**Trocar**, with blunt tip, size 6 mm, length 6 cm
3x 40123 NAL	**Trocar**, with blunt tip, flexible cannula, **autoclavable,** size 11 mm, working length 8.5 cm
2x 40120 NAL	**Trocar**, with blunt tip, flexible cannula, **autoclavable,** size 6 mm, working length 8.5 cm
43237 LGF	**CLICKLINE Parenchymal Forceps**, atraumatic, dismantling, without connector pin for unipolar coagulation, single action jaws, straight jaws, size 5 mm, length 28 cm
43237 LHF	**CLICKLINE Lung Forceps**, atraumatic, dismantling, without connector pin for unipolar coagulation, grasping distal end, single action jaws, single curved jaws, size 5 mm, length 28 cm
43244 LLP	**CLICKLINE Lung Forceps**, atraumatic, dismantling, without connector pin for unipolar coagulation, single action jaws, curved jaws, fenestrated, size 5 mm, length 28 cm
43244 LRP	**CLICKLINE Lung Nodule Forceps**, atraumatic, dismantling, without connector pin for unipolar coagulation, single action jaws, curved jaws, fenestrated, size 5 mm, length 28 cm
43231 LVS	**CLICKLINE Parenchymal Forceps**, atraumatic, dismantling, without connector pin for unipolar coagulation, single action jaws, curved jaws, size 5 mm, length 28 cm, for use with linear staplers
43249 LMP	**CLICKLINE Scissors**, dismantling, insulated, with connector pin for unipolar coagulation, double action jaws, curved scissor blades, size 5 mm, length 28 cm
43249 MTP	**CLICKLINE Scissors**, dismantling, insulated, with connector pin for unipolar coagulation, distally angled outer sheath, single action jaws, straight scissor blades, scissor blades open vertical to angulation, size 5 mm, length 28 cm
40170 LB	**Coagulation Suction Tube,** with connector pin for unipolar coagulation, distally angled sheath, size 5 mm, length 28 cm, for use with Handle 30804
30804	**Handle with Trumpet Valve,** for suction or irrigation, **autoclavable,** for use with 5 mm coagulation suction tubes, 3 and 5 mm suction and irrigation tubes
40360 LH	**Suction and Irrigation Tube,** with lateral holes, distally angled sheath, size 5 mm, length 28 cm for use with Handles 30805, 37112 A and 37113 A
30805	**Handle with Two-Way Stopcock,** for suction and irrigation, **autoclavable,** for use with suction and irrigation tubes size 5 mm
40775 LF	**Coagulating and Dissecting Electrode,** L-shaped, with connector pin for unipolar coagulation, distally angled sheath, size 5 mm, length 28 cm
26005 M	**Unipolar High Frequency Cord**, with 5 mm plug, length 300 cm, for use with AUTOCON® II 400 SCB system (111, 115, 122, 125), AUTOCON® II 200, AUTOCON® II 80, AUTOCON® system (50, 200, 350) and Erbe type ICC

Recommended Equipment for Cleaning, Sterilization and Storage

39219 XX	**Instrument Rack for Cleaning, Sterilization and Storage** of up to 14 instruments with diameter 2.5 to 10 mm, incl. variable bars with silicone holders, rack with Tray 39502 V for drawer and Wire Tray 39502 X, external dimensions (w x d x h): 480 x 250 x 125 mm
39752 A2	**Sterilization Container,** with MicroStop® microbiological barrier, for sterilization and sterile storage, external dimensions (w x d x h) 600 x 300 x 160 mm, internal dimensions (w x d x h): 548 x 267 x 138 mm
2x 39763 A2	**Coding label**, lettered, for use with sterilization container with 2x MicroStop®
2x 39762 A2	**Colour-flag**, black, for use with sterilization container with 2x MicroStop®

Notes:

with the compliments of
KARL STORZ — ENDOSKOPE